

# Impact of Lorentz Invariance Violation on the Propagation of Ultra-High-Energy Photons

---

**P. Morais,<sup>a,\*</sup> D. Boncioli,<sup>b,c</sup> F. Salamida,<sup>b,c</sup> I. P. Lobo<sup>a</sup> and V. B. Bezerra<sup>b</sup>**

<sup>a</sup>*Physics Department, Federal University of Paraíba,  
Caixa Postal 5008, 58059-900, João Pessoa, PB, Brazil.*

<sup>b</sup>*Università degli Studi dell'Aquila, Dipartimento di Scienze fisiche e chimiche, via Vetoio, L'Aquila, Italy*

<sup>c</sup>*Istituto Nazionale di Fisica Nucleare, Laboratori Nazionali del Gran Sasso, Assergi (AQ), Italy*

*E-mail:* [phm@academico.ufpb.br](mailto:phm@academico.ufpb.br)

This study explores how Lorentz invariance violation (LIV) affects photon interactions, both during intergalactic propagation (Breit-Wheeler process) and atmospheric interactions (Bethe-Heitler process). In the context of astroparticle propagation, we show how LIV can modify the cross section, the threshold energy, and consequently, the mean free path of particles. Shifting to atmospheric interactions, we analyze the impact of LIV on photon-initiated extensive air showers showing that the cross section of the initial interaction can be modified. Our results reveal that even small deviations from Lorentz invariance can lead to significant changes in both astroparticle propagation and photon dynamics. These findings enhance our understanding of high-energy astrophysical phenomena and open possibilities for testing quantum gravity theories.

*7th International Symposium on Ultra High Energy Cosmic Rays (UHECR2024)  
17-21 November 2024  
Malargüe, Mendoza, Argentina*

---

\*Speaker

## 1. Introduction

Exploring quantum gravity effects remains a major challenge, as these theories are difficult to be tested experimentally. Additionally, the limitation of experimental sensitivity to access the quantum gravity scale poses another significant challenge in capturing these effects [1–3]. To address these issues, quantum gravity phenomenology seeks to parametrize departures from fundamental aspects of Special/General Relativity from the semiclassical limit of quantum gravity.

Among these deviations, Lorentz Invariance Violation (LIV) emerges in several approaches to quantum gravity and represents an important window of investigation since Planck scale effects can be amplified when analyzing high-energy particle interactions [4–6].

High-energy multimessenger scenarios, including cosmic rays, gamma rays, neutrinos, and gravitational waves, provide the most effective tools for testing fundamental physics due to their high energy in the laboratory frame, comparable to ground-based accelerators. In this context, modifications due to LIV can influence various processes relevant to the production, propagation, and detection of these messengers.

In these scenarios, Modified Dispersion Relations (MDRs) frequently arise as a consequence of LIV, altering reaction kinematics based on the level of perturbation. These relations can be expressed in terms of energy as follows:

$$E^2 = m^2 + p^2 + m_{\text{eff}}^2, \quad (1)$$

where  $m_{\text{eff}}^2 = \sum_{n \geq 0} \eta_{i,n} \frac{E^{n+2}}{M_{Pl}^n}$  is the effective momentum-dependent masses of the particles,  $\eta_{i,n}$  represents the LIV coefficients, which in principle can be different for each type of particle,  $M_{Pl} = 1.22 \times 10^{19} \text{ GeV}^2$  is the Planck mass, and the velocity of low-energy photons is normalized to 1.

In this contribution, we will explore the propagation of photons in the extragalactic space and the Earth's atmosphere, by focusing separately on the modifications in the energy threshold for the relevant reactions as well as in the cross sections, in order to improve the analyses for testing LIV in UHE photons as already explored in [7, 8].

## 2. The effects of LIV in the extragalactic propagation

Photons produced in extragalactic space as a result of interactions between cosmic rays and background (CMB) or the extragalactic background light (EBL) are typically very high-energy photons (VHE) with  $E_\gamma = [10^9, 10^{22}] \text{ eV}$ . They can interact again with background photons – specifically those from the CMB and the radio background (RB), which have much lower energies, in the range  $\epsilon = [10^{-11}, 10] \text{ eV}$  – via the pair production process  $\gamma\gamma_{CMB} \rightarrow e^+e^-$ . In this interaction,  $\gamma$  represents the VHE photon with energy  $E_\gamma$ , with  $\gamma_{CMB}$  corresponding to the lower-energy photon with energy  $\epsilon$  from the CMB, producing electron-positron pairs and initiating an electromagnetic cascade.

Considering the cosmological effects as negligible, the optical depth,  $\tau(E_\gamma, z_s)$ , of the pair-production process is given by:

$$\tau_\gamma(E_\gamma, z_s) = \int_0^{z_s} dz \frac{dl(z)}{dz} \int_{-1}^1 d(\cos \theta) \frac{1 - \cos \theta}{2} \int_{\epsilon_{th}}^\infty \sigma(E_\gamma, \epsilon) n_\gamma(\epsilon, z) d\epsilon, \quad (2)$$

where  $\theta$  is the angle between the direction of propagation of both photons ( $\theta = [-\pi, +\pi]$ ),  $\sigma(E_\gamma, \epsilon)$  is the cross section of the interaction,  $\epsilon_{th}$  is the threshold energy of the interaction.

The distance traveled by a photon per unit redshift, at redshift  $z$ , is

$$\frac{dl(z)}{dz} = \frac{c}{H_0(1+z)\sqrt{\Omega_\Lambda + \Omega_M(1+z)^3}}, \quad (3)$$

where  $\Omega_\Lambda = 0.7$  is the dark energy density,  $\Omega_M = 0.3$  is the matter density,  $H_0 = 70 \text{ km s}^{-1} \text{ Mpc}^{-1}$  is the Hubble constant and  $c$  is the speed of light in vacuum.

We can therefore compute for a photon  $\gamma$  with energy  $E_\gamma$  and at a given redshift,  $z_s$ , the probability to reach Earth without interacting with the background as:

$$P_{\gamma \rightarrow \gamma}(E_\gamma, z_s) = e^{-\tau_\gamma(E_\gamma, z_s)}, \quad (4)$$

as suggested in [9].

LIV can manifest itself in the threshold energy of the process as well as in the cross section, which will be discussed in the next sections.

## 2.1 LIV modifications at the threshold energy

In order to incorporate LIV in the photon sector, as indicated in Eq. (1), the dispersion relation for VHE photons can be expressed as:

$$E_\gamma^2 - p_\gamma^2 = m_{\gamma, \text{eff}}^2, \quad (5)$$

where  $E_\gamma$  is the energy,  $p_\gamma$  is the momentum, and  $m_{\gamma, \text{eff}}$  is the effective mass of the VHE photon. For background photons, the energy is given by  $\epsilon = p_{\gamma_{CMB}}$ . Since their energy is significantly smaller than the Planck energy, the effects on their dispersion relations can be neglected. For electron-positron pairs, their dispersion relation follows the standard form:  $E_{e^\pm}^2 - p_{e^\pm}^2 = m_{e^\pm}^2$ .

To analyze how LIV impacts the interaction, we consider the conservation of energy and momentum, leading to the expression of the squared energy,  $s$ .

$$s = 2E_\gamma\epsilon(1 + \cos\theta) + m_{\gamma, \text{eff}}^2, \quad (6)$$

where the minimum energy required for the pair production is modified. For a head-on collision ( $\theta = \pi$ ) in Eq. (6), the threshold condition becomes:

$$\epsilon_{th} \geq \frac{4m_e^2 - m_{\gamma, \text{eff}}^2}{4E_\gamma}. \quad (7)$$

The variation of the threshold energy for different values of  $\eta$  (which enters in  $m_{\gamma, \text{eff}}$  for  $n = 1$ ) is illustrated in Fig. 1, demonstrating that the region where the process is allowed increases as  $\eta$  decreases.

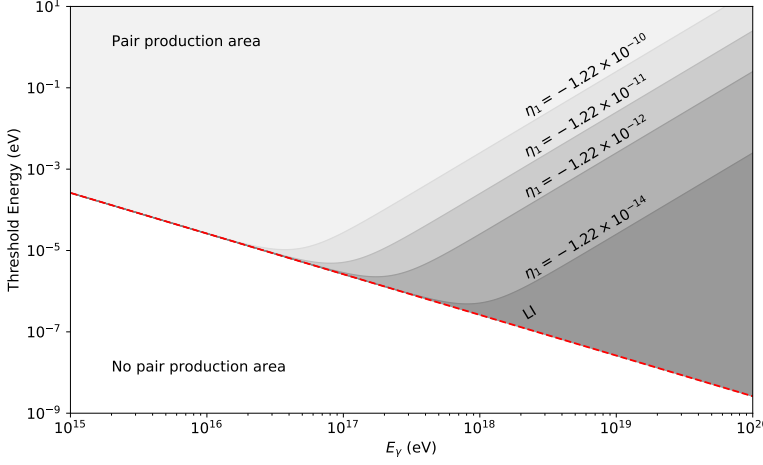


**Figure 1:** Threshold energy ( $\epsilon_{\text{th}}$ ) for pair production as a function of high-energy photon energy  $E_\gamma$ , showing allowed regions for different  $\eta$  values. Darker to lighter gray shades represent increasing  $\eta$  for  $n = 1$ , with the red dashed line for  $\eta = 0$  (LI case).

## 2.2 LIV modifications at the cross section

The cross section for the process  $\gamma\gamma_{CMB} \rightarrow e^+e^-$  is described by the Breit-Wheeler process and, in the standard case, can be written as:

$$\sigma_{BW}(E_\gamma, \epsilon) = \frac{\alpha^2 \pi}{2m_e^2} (1 - \beta^2) \left[ 2\beta(\beta^2 - 2) + (3 - \beta^4) \log \left( \frac{1 + \beta}{1 - \beta} \right) \right], \quad (8)$$

with  $\alpha = 1/137$ , and  $\beta$  is the velocity of the electron and positron in the center of mass reference frame  $\beta(E_\gamma, \epsilon) = \sqrt{1 - \frac{4m_e^2}{s}}$ .

Now, considering the aspects of LIV, we modify the cross section as described in [10]:

$$\sigma_{BW}^{LIV} = \frac{\alpha^2 \pi}{2E_\gamma \epsilon} \left( 1 + \left( 1 + \frac{m_{\gamma, \text{eff}}^2}{E_\gamma \epsilon} \right)^2 \right) \log \left( \frac{2E_\gamma \epsilon + m_{\gamma, \text{eff}}^2}{m_e^2} \right), \quad (9)$$

this expression is valid as long as the  $\eta$  parameter  $\eta \gg (m_e^2 - 2E_\gamma \epsilon) \frac{M_{Pl}^n}{E_\gamma^{n+2}}$ .

## 2.3 The modified mean free path in the extragalactic space

To calculate the mean free path  $\lambda_\gamma(E)$  in the local Universe, we initially neglect the cosmological effects of expansion. Instead, we use the photon mean free path,  $\lambda_\gamma(E)$ , to quantify the Universe's transparency rather than the optical depth. In this approach the survival probability for photons of energy  $E$  from a source at a redshift  $z$  can be approximated as  $P_{\gamma \rightarrow \gamma}(E_\gamma, D) \approx \exp(-D/\lambda_\gamma(E))$ , where  $D = cz_s/H_0$  is the distance from the source and the mean free path for the VHE photons is then given by

$$\frac{1}{\lambda(E_\gamma)} = \frac{\tau_\gamma(E_\gamma, DH_0/c)}{D}. \quad (10)$$

Next, to carry out the integration, it is more convenient to write the double integral as a function of the square center mass energy by performing a change of variables:

$$\frac{1 - \cos \theta}{2} = \frac{s - m_{\gamma, \text{eff}}^2}{4E_\gamma \epsilon} \quad \text{and} \quad d \left( \frac{1 - \cos \theta}{2} \right) = \frac{ds}{4E_\gamma \epsilon}, \quad (11)$$

the limits are now  $4m_e^2 < s < \infty$  and  $s/4E_\gamma < \epsilon < \infty$ , and assuming for  $z \ll 1$  the spectral density of CMB photons from [11] is given by

$$n_\gamma(\epsilon) = \epsilon/\pi^2(e^{\epsilon/kT_0} - 1)^{-1}, \quad (12)$$

then Eq. (10), take the form:

$$\frac{1}{\lambda_\gamma(E_\gamma)} = \frac{1}{8E_\gamma^2} \int_{4m_e^2}^{\infty} ds s \sigma_{\gamma\gamma}(s) \int_{s/4E_\gamma}^{\infty} d\epsilon \frac{n_\gamma(\epsilon)}{\epsilon^2}. \quad (13)$$

Now, we can use the dimensionless variables to simplify the numerical calculation,

$$\bar{s} = \frac{s}{4m_e^2}, \quad \bar{\epsilon} = \frac{\epsilon}{kT}, \quad \bar{E} = \frac{E_\gamma}{m_e^2/(kT)}, \quad (14)$$

where the product of the Boltzmann constant  $k$  and the temperature  $T$  of the CMB is  $kT = 2.35 \times 10^{-4}$  eV, and  $m_e^2 = 2.61 \times 10^{11}$  eV<sup>2</sup>. The new limits of integration in terms of the dimensionless variables are  $1 \leq \bar{s} \leq \infty$  and  $(\bar{s} - \frac{m_{\gamma,eff}^2}{4m_e^2})\bar{E}^{-1} = \bar{\epsilon}_{th} \leq \bar{\epsilon} \leq \infty$ .

Finally, the mean free path can be expressed in a simple form,

$$\frac{1}{\lambda_\gamma} = \frac{2(kT)^3}{\pi^2 \bar{E}^2} \int_1^{\infty} \left( \bar{s} - \frac{m_{\gamma,eff}^2}{4m_e^2} \right) d\bar{s} \int_{\bar{\epsilon}_{th}}^{\infty} \frac{d\bar{\epsilon}}{e^{\bar{\epsilon}} - 1} \sigma. \quad (15)$$

At this point, the only modifications in the mean free path are in the threshold energy and the modification of the squared energy from Eq. (6). Now, the cross section in Eq. (15) can be written considering the expression from Eq.(9), where we can assume a head-on collision. By writing it in terms of the dimensionless variables Eq. (14) the cross section is written as  $\sigma_{BW}^{LIV}(\bar{E}, \bar{\epsilon})$ . The results of LIV modification in the mean free path are shown in Fig. (2). The black line represents the mean free path in the standard scenario without LIV ( $\eta = 0$ ), indicating the SR. The colored curves illustrate the effects of LIV modifications for different values of  $\eta$ , with larger deviations observed for smaller values of  $\eta$  for  $n = 1$ . Notably, the mean free path increases significantly for high-energy photons as  $\eta$  decreases, demonstrating the suppression of photon interactions at ultra-high energies. This behavior highlights the sensitivity of the mean free path to both the LIV cross-section and threshold energy, emphasizing the impact of LIV on astrophysical photon propagation.

### 3. The impact of LIV in photon-initiated EAS

Primary ultra-high-energy (UHE) photons arriving at Earth interact with the atmosphere, resulting in extensive air showers. The most critical aspect of the shower development is the cross section of the first interaction. For energies around  $10^{18}$  and  $10^{19}$  eV the predominant interaction mechanism is the production of  $e^+e^-$  pairs on nitrogen nuclei in the atmosphere, known as the Bethe-Heitler (BH) process. Under standard conditions, the cross section for this process can be described as energy-independent as follows:

$$\sigma_{BH} = \frac{28Z^2\alpha^3}{9m_e^2} \left( \log \frac{183}{Z^{1/3}} - \frac{1}{42} \right), \quad (16)$$

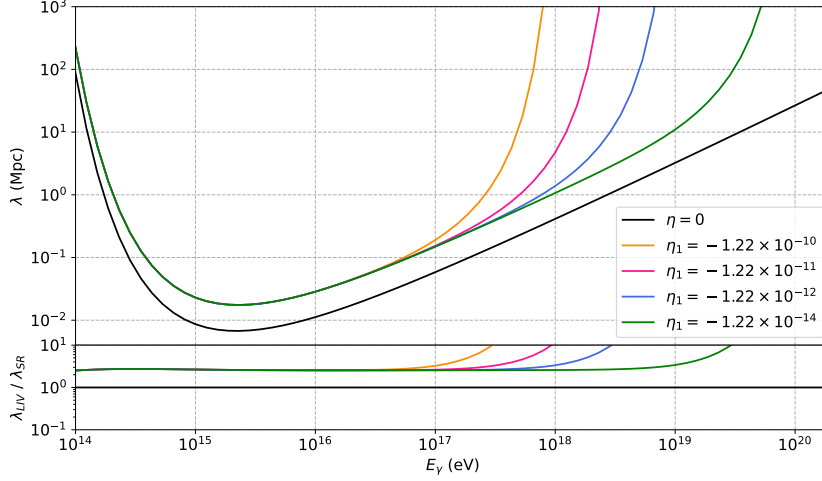


**Figure 2:** Mean free path for photons as a function of their energy in the range where the CMB is the relevant background. The black line curve corresponds to the mean free path in SR, and the colored curves represent the LIV scenarios with modifications in cross section and threshold with different values of  $\eta$  and  $n = 1$ .

where  $m_e$  is the electron mass,  $\alpha = 1/137$  is the atomic number, and  $Z$  is the atomic number of the target nucleus. Considering nitrogen ( $Z = 7$ ) as the target, the cross section is  $\sigma_{BH} \approx 500$  mb. Now, if we consider the effects of LIV as from MDR in Eq. (1), the modified cross section studied in [10, 12] takes the form:

$$\sigma_{BH}^{LIV} = \frac{8Z^2\alpha^3}{3|m_{\gamma,\text{eff}}^2|} \log \frac{1}{\alpha Z^{1/3}} \log \frac{|m_{\gamma,\text{eff}}^2|}{m_e^2}, \quad (17)$$

where the  $|m_{\gamma,\text{eff}}^2|$  is the effective momentum-dependent mass, and the cross section validity is determined by the condition  $|m_{\gamma,\text{eff}}^2| \gg m_e^2$  according to [12], which results in

$$|\eta| \gg m_e^2 \frac{M_{Pl}^n}{E^{n+2}}. \quad (18)$$

The probability for a photon to produce a pair in the atmosphere, as shown in [13], can be written as,

$$P = \int_0^{X_{\text{atm}}} dX_0 \frac{e^{-X_0/\langle X_0 \rangle_{LIV}}}{\langle X_0 \rangle_{LIV}} = 1 - e^{-X_{\text{atm}}/\langle X_0 \rangle_{LIV}}, \quad (19)$$

where the mean depth of interactions  $\langle X_0 \rangle_{LIV}$  in the LIV case can be expressed via the mean depth  $\langle X_0 \rangle_{LI} = 57 \text{ g cm}^{-2}$  in the LI case and the ratio of the cross sections  $\sigma^{LIV}$  and  $\sigma^{LI}$  as follows:

$$\langle X_0 \rangle_{LIV} = \frac{\sigma^{LI}}{\sigma^{LIV}} \langle X_0 \rangle_{LI}. \quad (20)$$

Using the Eq. (20) in the equation Eq. (19), we can write the probability in terms of the  $|m_{\gamma,\text{eff}}^2|$  in the following way:

$$P(E_\gamma, \eta) = 1 - \exp \left( -0.298 \times \frac{X_{\text{atm}}}{57 \text{ g cm}^{-2}} \frac{m_e^2}{|m_{\gamma,\text{eff}}^2|} \log \frac{|m_{\gamma,\text{eff}}^2|}{m_e^2} \right). \quad (21)$$

The probability  $P(E_\gamma, \eta)$  is interpreted as a suppression factor for assuming the potential of particle shower formation.

The prediction for the observed flux as formulated in [13] is therefore:

$$\left(\frac{d\Phi}{dE}\right)_{\text{LIV}} = P(E_\gamma, \eta) \times \frac{d\Phi}{dE}\Bigg|_{\text{source}}, \quad (22)$$

where the suppression factor is given by Eq. (21). The effect of atmospheric suppression on the simulated UHE photon flux is shown in Fig.(3b), in contrast to Fig.(3a), which does not account for atmospheric suppression. The results show that including the suppression of atmospheric shower production reduces the expected photon flux, aligning the curves with the measured upper limits from the Pierre Auger Observatory for the studied values of  $\eta$ . This suggests that these values of  $\eta$  cannot be excluded.

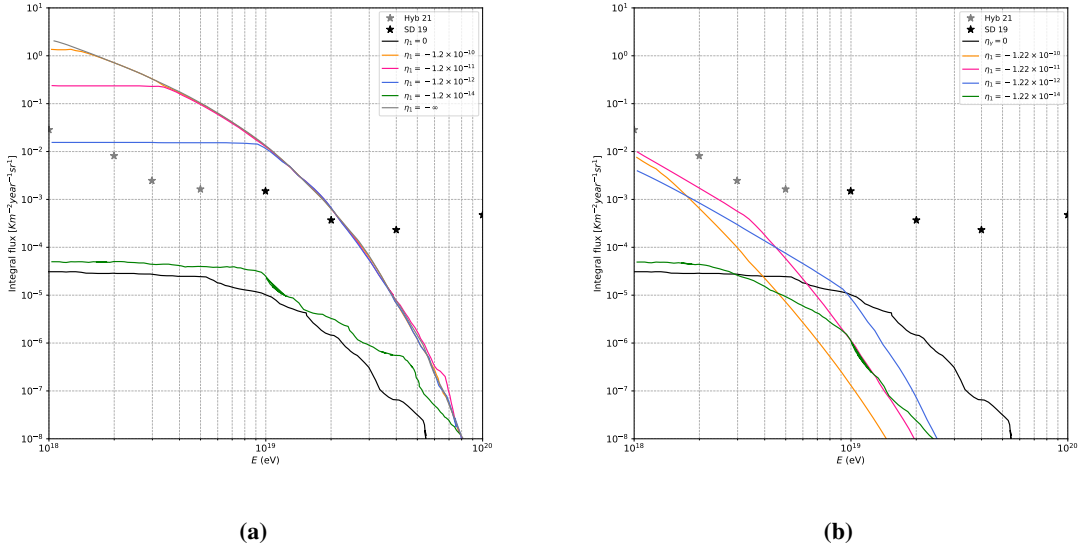


**Figure 3:** The simulated integral flux of UHE photons as a function of the energy. Left: simulated integral fluxes as taken from [7] with LIV effects only in the intergalactic propagation. Right: same simulated integral fluxes, including the atmospheric suppression as calculated in this work.

#### 4. Conclusion

In this work, we explore the effects of LIV on the propagation of UHE photons in extragalactic space and their interaction in Earth's atmosphere. We analyze how LIV modifies both the cross-section and threshold energy for the BW and BH processes. Although LIV increases the number of UHE photons reaching Earth, it also suppresses the formation of particle showers in the atmosphere. Although the constraints on LIV parameters become less strict when accounting for atmospheric suppression, the results are more robust as they include LIV effects in both propagation and detection stages.

## References

- [1] G. Amelino-Camelia, C. Lammerzahl, A. Macias, and H. Muller. The Search for quantum gravity signals. *AIP Conf. Proc.*, 758(1):30–80, 2005. doi: 10.1063/1.1900507.
- [2] Lee Smolin. How far are we from the quantum theory of gravity? 3 2003.
- [3] Rodrigo Guedes Lang, Humberto Martínez-Huerta, and Vitor de Souza. Ultra-High-Energy Astroparticles as Probes for Lorentz Invariance Violation. *Universe*, 8(8):435, 2022. doi: 10.3390/universe8080435.
- [4] Giovanni Amelino-Camelia. Quantum-Spacetime Phenomenology. *Living Rev. Rel.*, 16:5, 2013. doi: 10.12942/lrr-2013-5.
- [5] A. Addazi et al. Quantum gravity phenomenology at the dawn of the multi-messenger era—A review. *Prog. Part. Nucl. Phys.*, 125:103948, 2022. doi: 10.1016/j.pnpnp.2022.103948.
- [6] R. Alves Batista et al. White Paper and Roadmap for Quantum Gravity Phenomenology in the Multi-Messenger Era. 12 2023.
- [7] Pedro Abreu et al. Testing effects of Lorentz invariance violation in the propagation of astroparticles with the Pierre Auger Observatory. *JCAP*, 01(01):023, 2022. doi: 10.1088/1475-7516/2022/01/023.
- [8] Humberto Martínez-Huerta, Rodrigo Guedes Lang, and Vitor de Souza. Lorentz Invariance Violation Tests in Astroparticle Physics. *Symmetry*, 12(8):1232, 2020. doi: 10.3390/sym12081232.
- [9] Alessandro De Angelis, Giorgio Galanti, and Marco Roncadelli. Transparency of the Universe to gamma rays. *Mon. Not. Roy. Astron. Soc.*, 432:3245–3249, 2013. doi: 10.1093/mnras/stt684.
- [10] Grigory Rubtsov, Petr Satunin, and Sergey Sibiryakov. Calculation of cross sections in lorentz-violating theories. *Phys. Rev. D*, 86:085012, Oct 2012. doi: 10.1103/PhysRevD.86.085012. URL <https://link.aps.org/doi/10.1103/PhysRevD.86.085012>.
- [11] D. J. Fixsen, E. S. Cheng, J. M. Gales, John C. Mather, R. A. Shafer, and E. L. Wright. The Cosmic Microwave Background spectrum from the full COBE FIRAS data set. *Astrophys. J.*, 473:576, 1996. doi: 10.1086/178173.
- [12] Grigory Rubtsov, Petr Satunin, and Sergey Sibiryakov. Prospective constraints on Lorentz violation from ultrahigh-energy photon detection. *Phys. Rev. D*, 89(12):123011, 2014. doi: 10.1103/PhysRevD.89.123011.
- [13] Petr Satunin and Andrey Sharofeev. Shower formation constraints on cubic Lorentz invariance violation parameters in quantum electrodynamics. *Eur. Phys. J. C*, 84(8):793, 2024. doi: 10.1140/epjc/s10052-024-13152-3.